MECHANICAL BEHAVIOR OF SMAHC BARS AND BEAMS TESTED AT TWO DIFFERENT TEMPERATURES

Flaminio Levy Neto, flaminio@unb.br
Peter Faluhelyi, pyi@brturbo.com.br
Universidade de Brasília, UnB-FT-ENM, 70910-900, Brasília, DF, Brasil
Edson Paulo da Silva, dasilva@em.ufop.br
Universidade Federal de Ouro Preto, UFOP- Escola de Minas, 75400-000, Ouro Preto, MG, Brasil

Abstract. *Adaptative or smart composite structures, incorporating Ni-Ti Shape Memory Alloys (SMA), is an attractive research topic in engineering. This work is concerned with the fabrication as well as the mechanical behavior of hybrid composite structures, in the form of epoxy matrix bars and beams, reinforced with E-glass chopped mat as well as functional Ni-Ti wires, subjected to static loads and tested at two different temperatures: T=25°C<Tm; and T=69°C>Ta. For T<Tm Ni-Ti presents martensitic phase, whereas for T>Ta it is fully converted in the austenitic phase and its elasticity modulus increases by a factor greater than two. This significant change in the elasticity modulus of Ni-Ti alloy have motivated the application of such alloys for structural and machine vibration control. One way to explore the special behavior of SMA for vibration control, in practical situations, is the concept of Shape Memory Alloy Hybrid Composites (SMAHC). The specimens tested in the present investigation, in particular the composite beams, showed a change up to 10% in stiffness, when the temperature of the wires varied from 25°C to 69°C. The results indicate that such SMAHC components can be explored in vibration control, particularly to avoid dangerous forced vibrations to take place.*

Keywords*: Smart structures, shape memory alloys, stiffness control.*

1. INTRODUCTION

Composite materials combine synergistically at least two distinct phases, normally at macroscopic scale, and are well known by their high specific strength as well stiffness, which allow the creation of efficient and light structural components (Daniel and Ishai, 2006; Levy-Neto and Pardini, 2006). The continuous phase, the matrix, agglutinates and protects the reinforcement, mostly in the form of high performance fibers like E-glass, aramid and carbon. The composites investigated in the present study, designated by Rogers and Robertshaw (1989) as *Shape Memory Alloy Hybrid Composites (SMAHC)*, are bars and beams that incorporate a third constituent, Ni-Ti wires, which is a functional material itself. The development of Ni-Ti shape memory alloys (SMA) has paved the way for special applications in robotics, bioengineering and complex aerospace systems, where multiple functions, as sensor and actuator, are required (Ghandi and Thomson, 1992; Janocha, 1999; Srinivasan and McFarland, 2001). With the addition of the Ni-Ti wires, which besides other features increase their elasticity modulus when heated, SMAHC can be regarded as adaptative or smart structures. The development of smart/intelligent composite structures, incorporating SMA, has become an attractive research topic in engineering and applied sciences due to their capacity to work as a sensor or actuator (Turner, 2000).

Adaptative composite structures with embedded Ni-Ti wires, among other features, are able to respond to external inputs and commands, for example a moderate increase in temperature (e.g. from 25 °C to 69 °C). These SMA wires are able to change their elasticity modulus, by a factor of almost three times, as showed in Fig. 1 and recover from pseudoplastic deformations up to 8%, when a controlled electric current warms up the wires (Srinivasan & McFarland, 2001). Thus, the same SMAHC component can present different mechanical behavior and adapt itself to service and environmental conditions. The shape memory and pseudoelasticity phenomena presented by SMA, for instance the Ni-Ti alloys, have motivated the application of such special alloys in many situations, for structural as well as machine vibration control and the optimization of different mechanical systems (Otsuka and Wayman, 1998).

The special properties presented by the Ni-Ti alloys depends on the transformation of the crystal structure, from the relatively softer martensitic phase, at lower temperatures (e.g. T < 25 ºC), to the stiffer austenite phase at higher temperatures (e.g. T > 69 ºC). During the initial development of Ni-Ti alloys, it was found that a composition consisting of equal numbers of nickel and titanium atoms showed the transformation that leads to shape memory and an increase on the elasticity modulus (E). Further, by adding a slight extra amount of nickel in the alloy, it was possible to change the transformation temperature from near 100 ºC down to below 0 ºC. Also, this alloy had constituents that were not prohibitively expensive, had greater shape memory strain and could be produced with existing metalworking techniques. The important temperatures at which phase transformations take place are known as: $\boldsymbol{M_s}$; $\boldsymbol{M_f}$; $\boldsymbol{A_s}$; as well as $\boldsymbol{A_f}$, and represent the temperatures of start (s) and finish (f) of martensitic (M) and austenitic (A) transformations, respectively (Srinivasan and McFarland, 2001). They can be determined precisely using a calorimeter, but an approximate estimation can be obtained by monitoring practically any property of the alloy, for instance its electrical

resistance (Turner, 2000). The main effect that is explored at the present work is the significant variation of the elasticity modulus (E) of the Ni-Ti wires, from E_M , at $T < \boldsymbol{M_s}$ in the martensitic phase, up to $E_A \cong 3.E_M$ (i.e. almost three times larger), at $T > \mathbf{A_f}$ in the austenitic phase (Turner, 2000), as presented in Fig. 1. Thus, since the natural frequency of a structural component depends on its mass and stiffness, this frequency, in a SMAHC with embedded Ni-Ti wires, can be changed controlling the temperature of the wires. Meanwhile, the fabrication of SMAHC is complex due to the fact that it involves three different constituents integrated in the same component. In view of this scenario, the main objectives of this work are: (i) the development of a feasible fabrication method to produce 13 SMAHC specimens: four beams and nine bars; and (ii) evaluate the elastic properties of SMAHC bars and beams with different volume fractions of Ni-Ti wires, subjected to static loads, at 25 °C (i.e. $T < \boldsymbol{M_f}$) and to 69 °C (i.e. $T > \boldsymbol{A_f}$).

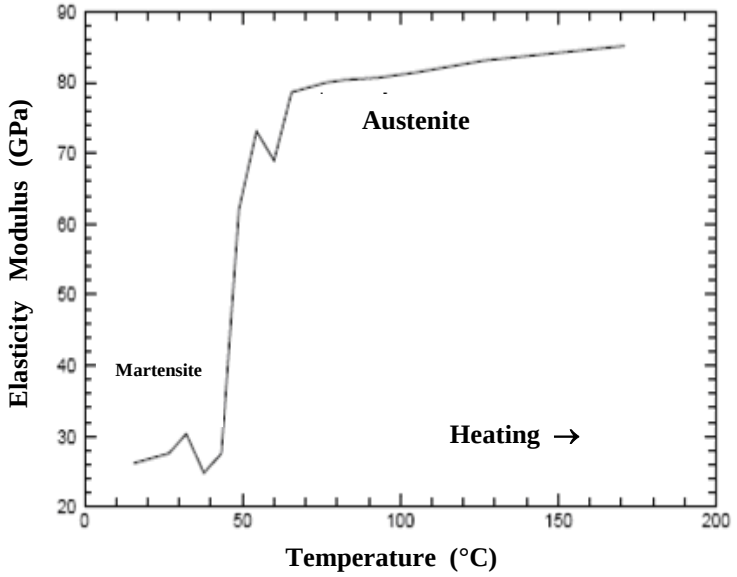

Figure 1. Elasticity Modulus of a Ni-Ti wire from $T < M_f$ up to $T > A_f$ (Turner, 2000).

2. MATERIALS AND METHODS

2.1. General aspects concerning the fabrication process of SMAHC bars and beams

Due to its simplicity and low cost, the hand lay up process, without vacuum bag, with consolidation inside closed moulds (i.e. male and female combined), was chosen for the fabrication of the SMAHC bars (nine) and beams (four) investigated in this work. The constituents adopted were: (i) cold cure (25°C) and hot cure (80 °C) epoxy resins from Maxepoxi; (ii) E-glass chopped fibers mat; and (iii) Ni(55.5%)–Ti(44.5%) wires from Memry GmbH, washed with the reagent Kroll (Faluhelyi, 2010). The basic geometry of the specimens was based on the ASTM standards D 3039-08, for the bars and D 790-07, for the beams. In both cases, an external steel device to keep the Ni-Ti wires stretched during the consolidation of the epoxy matrix was attached to an internal aluminum female mould, as illustrated in Fig. 2.

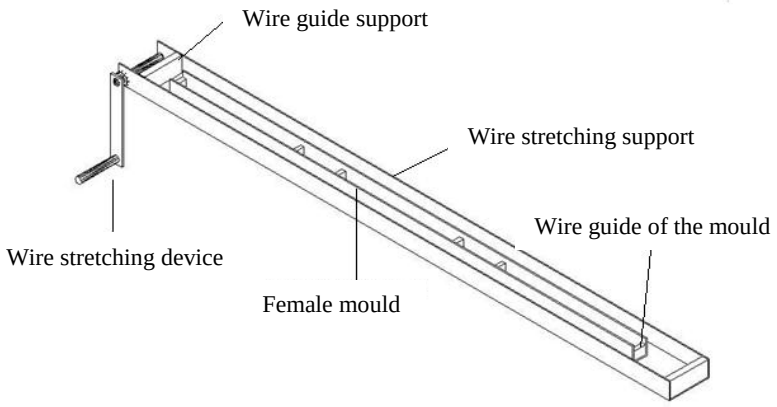

Figure 2. Stretching device and female mould.

The female mould presented in Fig. 2 is 1200 mm long and endowed with sets of blocks with uniformly distributed holes to guide the Ni-Ti wires. It is an U shape aluminum bar, with internal width of 31.3 mm, which is fixed on the steel base wire stretching support. In the beginning of the fabrication of the bars and beams, one extremity of the wires is fixed in a guiding block and the other end is griped and pulled by the lever of the stretching device. Thus, during the lamination of the E-glass/epoxy plies, the wires are kept straight until the resin is totally cured. As far as the cure temperature of the matrix is concerned, the specimens were divided into two main groups: cold (25°C) and hot (80°C) cure. For the cold cure group the epoxy system LY1316/HY1208 (glass transition temperature Tg = 60°C) was used to impregnate the E-glass mat and Araldite-F/HY956 (Tg = 80°C) to impregnate the wires; whereas for the hot cure group the system LY1316/HY1316 (Tg > 80°C) was adopted for all the layers. The cure cycle for the cold system is single stage, 24 hours at 25 °C (i.e. room temperature); and for the hot system two stages, with pre cure at room temperature for 10 hours, followed by a post cure at 80 °C for 7 hours. Initially, the layers of E-glass mat (450 g/m^2), as well as the wires, are cut and weighted in a digital scale and their total mass, $\mathbf{m_f}$ and $\mathbf{m_w}$, respectively, are registered. When the specimens are extracted from the moulds their total weight, $\mathbf{m_T}$, is measured. With these values it is possible to calculate the mass of matrix, $\mathbf{m_m}$, and the respectively mass fractions of matrix, fibers and wires. In addition, with the densities of the constituents it is possible to obtain the respective volume fractions, $\mathbf{V_f}$, $\mathbf{V_w}$ and $\mathbf{V_m}$.

2.2. Fabrication of the SMAHC beams for the bending tests

The SMAHC beams are fabricated directly in the U shape female mould, which was previously covered with a layer of release wax. The typical cross section of the beams, with the geometric details incorporated, is presented in Fig. 3. The symmetric lamination starts with two (2) layers of E-glass mat/epoxy, followed by one (***1***) layer Ni-Ti /epoxy and thirteen (13) E-glass/epoxy plies. And, since the stacking sequence is symmetric about the beams middle surface (i.e. at t/2), the last layers of Ni-Ti/epoxy and E-glass/epoxy have the same materials and thickness as the initial one (i.e. the number of plies, in sequence, is: 2+***1***+13+***1***+2, where the symmetric Ni-Ti layers are represented in bold and italic). Figure 3 refers to a beam with 8 Ni-Ti wires, 4 above the middle surface and 4 below. The nominal length of all the six beams manufactured in this work was L = 300 mm and the width 31.3 mm.

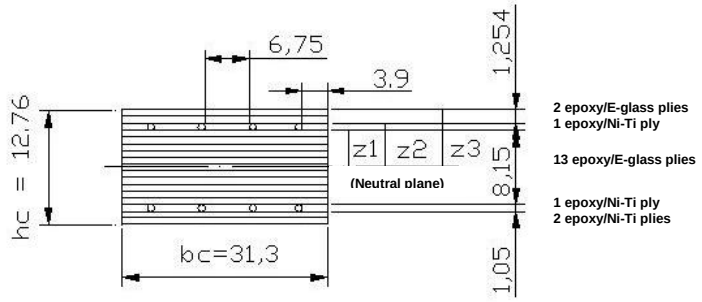

Figure 3. Cross-section view of the SMAHC beam (dimensions in mm).

The first two beams were fabricated without wires and consisted of 16 layers of E-glass/epoxy. Since the Ni-Ti SMA is very expensive, costing about US$ 1000/kg, in the next two specimens 8 wires of special galvanized alloy (SGA) were used, 4 above the midplane and 4 below, mainly to get experience in the manufacturing process which is rather complex and need two well trained operators. The nominal diameter of the SGA wires was 0.89 mm. Finally, the last two beams, incorporating symmetric layers reinforced with Ni-Ti wires of nominal diameter 1.05 mm, as presented in Fig. 3, were manufactured. The total thickness and mass of the beams, as well as the volume fractions of the constituents (i.e. $\mathbf{V_f}$, $\mathbf{V_w}$ and $\mathbf{V_m}$) are presented in Table 1.

Table 1. Identification and main characteristics of the beams reinforced with E-glass, SGA and Ni-Ti.

Beam	Characteristics	Average thickness (mm)	Standard Deviation (mm)	Total mass (grams)	$\mathbf{V_f}$ %	$\mathbf{V_w}$ %	$\mathbf{V_m}$ %
1	Without wires/cold cure	13,73	0,39	228	23	-	77
2	8 SGA wires/cold cure	11,86	0,24	200	21	1	78
3	8 Ni-Ti wires/cold cure	12,45	0,60	180	26	1.7	72.3
4	8 Ni-Ti wires/hot cure	12,76	0,32	182	25	1.8	72.2

2.3. Fabrication of the SMAHC bars for the tensile tests

In the fabrication of the nine SMAHC symmetric bars all the Ni-Ti wires were located at the middle surface plane of the specimens and the number of wires varied from 2 to 8. As for the SMAHC beams, depending on the cure temperature, the bars were divided into two main groups: cold (25°C, 24 hours) and hot (25°C, 10 hours, followed by 7 hours at 80°C) cure. For the single stage cold cure group the epoxy system LY1316/HY1208 (Tg = 60°C) was used to impregnate the E-glass mat and Araldite-F/HY956 (Tg = 80°C) to impregnate the wires; whereas for the hot cure group the system LY1316/HY1316 (Tg > 80°C) was adopted for all the layers.

Before the lamination of the bars the male tool illustrated in Fig. 4 was installed on the bottom surface of the same U shape aluminum female mould used for the fabrication of the beams. In addition, in order to produce the specimens with the shape shown in Fig. 5, another tool, flipped vertically relatively to the one presented in Fig. 4, was attached to the male mould. The six E-glass mat central layers, which correspond to the prismatic testing zone of the specimens (i.e. with constant rectangular cross-section), were 265 mm long; whereas for the tabs and including the inclined transition between the testing zone and the tabs, 4 sets of 7 strips of E-glass mat, 42, 47, 50, 53, 56, 59 e 62 mm long, were cut, in order to produce a smooth transition. Since the bars are symmetric about the middle surface, the stacking sequence of the plies, in the tabs, was: 7+3+***1***+3+7, where the single Ni-Ti at the middle surface is represented in bold and italic. Details about the 12 SMAHC bars are shown in Table 2.

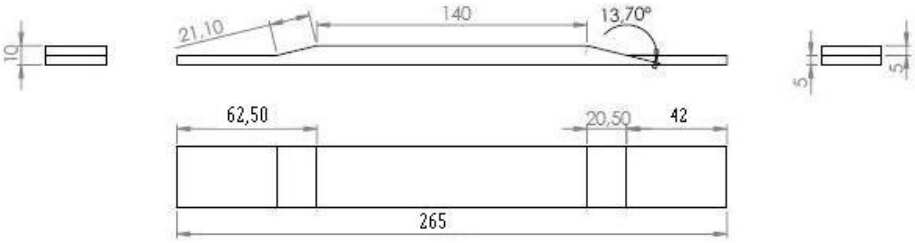

Figure 4. Side view and top view of the bars male tool (dimensions in mm).

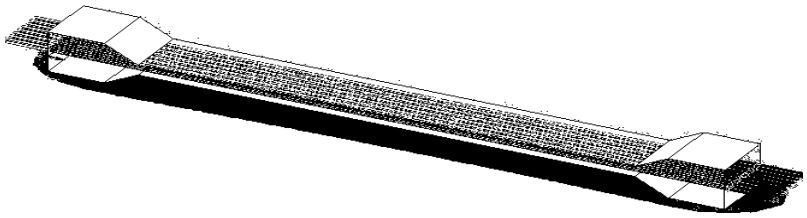

Figure 5. Isometric approximate view of the SMAHC bars (i.e. not in scale).

Table 2. Identification and main characteristics of the bars reinforced with E-glass, SGA and Ni-Ti

bars	Characteristics	Average thickness (mm)	Standard deviation (mm)	$\mathbf{V_f}$ %	$\mathbf{V_w}$ %	$\mathbf{V_m}$ %
1	Without wires/cold cure	3.89	0.15	28.0	-	72.0
2	8 SGA wires/cold cure	3.23	0.43	23.2	5.29	71.5
3	2 Ni-Ti wires/cold cure	4.66	0.17	22.2	1.17	76.6
4	2 Ni-Ti wires/hot cure	5.06	0.08	21.0	1.11	77.9
5	4 Ni-Ti wires/cold cure	4.41	0.09	22.9	2.44	74.7
6	4 Ni-Ti wires/hot cure	4.68	0.24	22.7	2.40	74.9
7	8 Ni-Ti wires/cold cure	3.89	0.04	32.8	6.93	63.0
8	8 Ni-Ti wires/hot cure	3.76	0.41	27.1	5.87	67.0
9	8 Ni-Ti wires/hot cure	3.65	0.17	27.9	6.04	66.0

The prismatic test section of the bars (i.e. the gage length) was 140 mm long and 31.3 mm wide. The thicker tabs at both extremities of the bars are a strict recommendation of the ASTM standard D 3039-08 in order to protect the brittle specimens from the jaws of the MTS-810 during the tensile tests.

2.4. Physical and mechanical characterization of the materials and specimens

Most of the physical and mechanical properties of the materials employed in this work (i.e. epoxy resin, E-glass fibers as well as special galvanized alloy (SGA) and Ni-Ti wires) were obtained from the literature (Daniel and Ishai, 2006; Levy-Neto and Pardini, 2006; Janocha, 1999; Srinivasan and McFarland, 2001) and from the catalogs of the manufacturers of the products. The mass and average diameter of 1 m long Ni-Ti wires was measured. In addition, the elasticity modulus (E) and tensile strength of 150 mm long Ni-Ti wires with glass/epoxy tabs, in the martensitic (E_M) and austenitic (E_A) phases, tested in a MTS-810 machine, at 25 °C and 69 °C, respectively, were obtained experimentally. The density, elasticity modulus and tensile strength of the materials used are presented in Table 3. As explained in section 2.5, in order to increase the temperature of the wires to 69 °C a controlled electric current is applied on them, using schematic setup presented in Figure 6. A closed loop electronic circuit that measures the temperature and controls the current was developed for this purpose (Cerón, 2010). It is working well only when the stretched wire is in the elastic regime and reductions in the cross section area are still negligible. In addition, the test machine is metallic, conducts electricity and the jaws that hold the wires must be well insulated from the leads, which apply the electric current on them. Some improvements on the insulation are still needed and in course.

Table 3. Physical and mechanical properties of the materials.

Material	Density (g/cm^3)	Elasticity Modulus (GPa)	Tensile Strength (MPa)
Special galvanized alloy (SMA) wires	6.37	75	500
E-glass fibers	2.54	70	2400
Epoxy resin (LY1316/HY1208)	1.05	3.3	55
Ni-Ti wires/Martensitic phase	6.45	22.6	750
Ni-Ti/Austenitic phase	6.45	48.4	930

2.5. Heating and electric characterization and heating of the Ni-Ti wires

In order to apply and control the electric current on the Ni-Ti wires, they were assembled in series and connected to a 12 volts D.C. power unit, as shown in Fig. 6. Details about the on-off control system can be found in Sandoval (2010). The heating system represented in Fig. 6 is based on the Joule effect and was used to control the temperature of single Ni-Ti wires as well as SMAHC bars and beam. In the bars and beams the embedded wires are connected in series. Thus the same electric current flows throughout all the Ni-Ti wires.

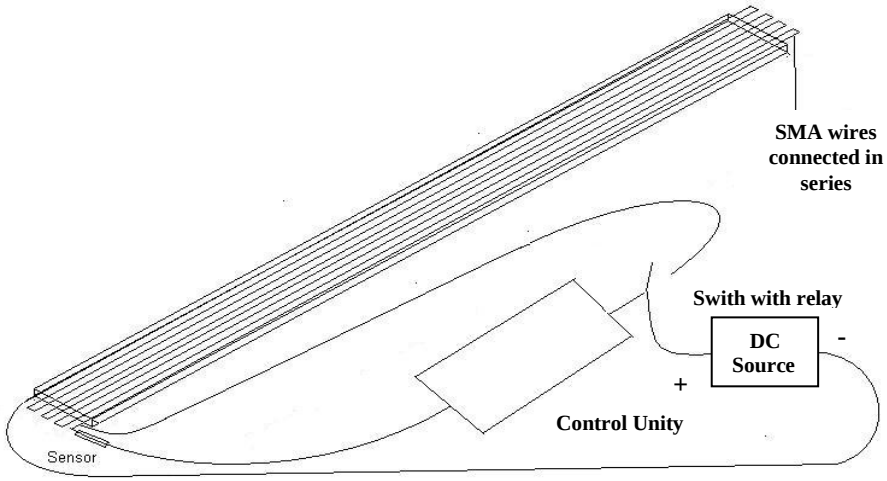

Figure 6. Schematic view of the electrical system to heat the Ni-Ti wires.

2.6. Mathematical modeling of the SMAHC beams in bending and bar in tension

In order to analyze the bending stiffness of a composite beam with functional SMA wires as well as structural fibers embedded in an epoxy matrix material, it is necessary to account for the effect of the Ni-Ti on the elastic properties of the SMAHC and for its main role to increase the effective flexural modulus ($\mathbf{E_F}$), during the phase transformation from martensite (E_M) to austenite ($E_A \cong 2.E_M$, in this work). Because the epoxy resin is an excellent adhesive and the Ni-Ti wires are strait and parallel to the longitudinal direction it is natural to treat them as unidirectional reinforcement in the matrix of composite material whose properties are known. This allows the use of classical lamina and laminate macromechanical equations (Gibson, 1994; Levy Neto and Pardini, 2006) to estimate the influence of Ni-Ti wires volume fraction and placement, along z direction, on the flexural modulus ($\mathbf{E_F}$), in particular Eq.(1) for symmetric laminated beams. The representation of such beams is shown in Figs. 3 and 7, where x is the longitudinal axis and z the vertical distance from the middle surface of the beam. Using Eq. (1) deflections of SMAHC beams can be calculated by using $\mathbf{E_F}$ in place of the elasticity modulus (E) in the beam deflections equations from elementary mechanics of materials (Gibson, 1994).

$$E_F = \frac{8}{t^3} \cdot \sum_{j=1}^{N/2} (E_x)_j \cdot (z^3{}_j - z^3{}_{j-1}) \tag{1}$$

where: t is the total thickness of the beam; N is the total number of plies; j is the index of each ply and varies from 1 to N ($1 \le j \le N$); $\mathbf{(E_x)_j}$ is the elasticity modulus of each ply in the longitudinal direction x of the beam; and z is the vertical distance measured from the middle surface of the beam (i.e. at t/2).

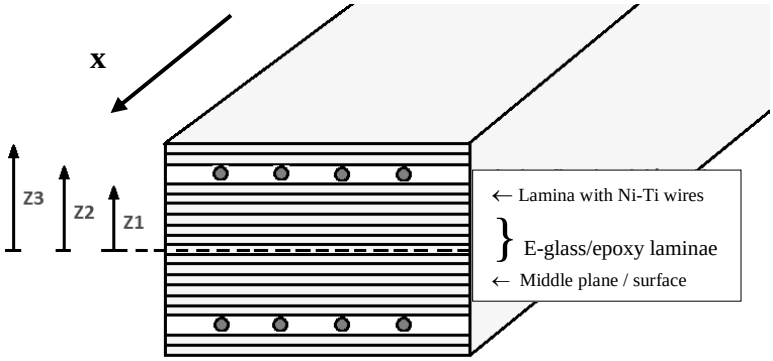

Figure 7. Schematic representation of a symmetric laminated SMAHC beam.

The elasticity modulus of the composite layers $\mathbf{(E_x)_j}$ were calculated using Eq. (2) obtained from Mendonça (2005), for the plies of E-glass chopped mat/epoxy (E_{GE}); and from the rule of the mixtures, Eq. (3), given by Daniel and Ishai (2006), combined with Eq. (2), for the layers reinforced with Ni-Ti wires (E_{SMA}).

$$E_{GE} = 3.44 + 28.2\, V_f + 21.6\, V_f^4 \tag{2}$$

where: V_f is the volume fraction of chopped E-glass fibers in the E-glass/epoxy plies.

For the layers of Ni-Ti/epoxy in particular the SMA wires can be modeled as unidirectional reinforcement and the resulting longitudinal elasticity modulus ($E_{SMA/E}$) can be calculated using Eq. (3), based on the micromechanics approach (Gibson, 1994), since the Ni-Ti wires (E_{SMA}) and the matrix (E_m) are subjected to the same longitudinal strain.

$$E_{SMA/E} = E_{SMA} \,.\, V_{SMA} + E_m \,.\, V_m \tag{3}$$

where: V_{SMA} and V_m are the volume fractions of wires (SMA) and matrix (m) in these particular plies.

Finally, since the E-glass/epoxy plies (E_{GE}) as well as the layers reinforced with SMA wires ($E_{SMA/E}$) are parallel to each other and subjected to the same strain in tension, the longitudinal elasticity modulus of the bars (E) can be calculated from Eq. (4) according to the rule of mixtures (Gibson, 1994):

$$E = E_{GE} \,.\, V_{GE} + E_{SMA/E} \,.\, V_{SMA/E} \tag{4}$$

where: V_{GE} and $V_{SMA/E}$ are the volume fractions of E-glass/epoxy and SMA/epoxy plies in the bars.

3. EXPERIMENTAL AND THEORETICAL RESULTS

The beams were tested in three points bending, following ASTM Standard D 790-07, under static loads in the elastic regime at 25 °C and 69 °C. The loads (P), at a rate of 1 mm per minute, were applied at the midspan (L/2), using the MTS 810 machine. In all the tests the span (distance between the supports at the extremities) was L = 114 mm and the maximum deflection (δ) was given by Eq. (5). The maximum deflection was kept below L/10 in all tests. Thus, from the values of P and δ, obtained from the MTS machine, as well as L and I, it was possible to obtain E_F experimentally. In addition, using Eq. (1), was possible to calculate E_F theoretically. These results are presented in Table 4.

$$\delta = (P \,.\, L^3) \,.\, (48.\, E_F \,.\, I)^{-1} \tag{5}$$

where: P is the applied load; L is the span of the beam; $I = (b.t^3)/12$ is the moment of inertia of the cross section of the beam measured from the middle surface; t is the total thickness obtained from Table (1) and b=31.3 mm is the width of the beams. For the beams 3 and 4 tests were carried out with the Ni-Ti wires at 25 °C and 69 °C.

The bars were tested in tension under static loads, in the elastic regime at 25 °C and 69 °C, following ASTM Standard D 3039-08, as shown in Fig. 8. The longitudinal elasticity moduli of the bars were obtained experimentally, using the MTS-810 machine and calculated analytically using Eq. (4). These results are presented in Table 5.

Table 4. Experimental and theoretical results for flexural elastic properties of the SMAHC beams.

Beams/ (Ni-Ti phase)	Theoretical flexural modulus, E_F Eq. (1)	Experimental flexural modulus[(1)]	Percentage differences[(2)]
	E_F (GPa)	E_{Exp} (GPa)	(%)
1 (no wires)	11.70	7.55	+54.97
2 (SGA wires)	9.98	7.82	+27.62
3 (martensitic, 25 °C)	8.62	8.40	+ 2.62
3 (austenitic, 69 °C)	9.53	9.37	+ 1.71
4 (martensític, 25 °C)	8.82	8.60	+ 2.56
4 (austenitic, 69 °C)	9.54	9.38	+ 1.71

(1) at 25 ºC and 69 ºC for beams 3 and 4, with martensític and austenitic phase of Ni-Ti wires, respectively.
(2) percentage values were calculated using the expression: $(E_{Theo} - E_{Exp} / E_{Exp}) \times 100$.

Figure 8. Tensile test of a SMAHC bar at 69 °C (Ni-Ti in the austenite phase)

Table 5. Experimental and theoretical results for tensile elastic properties of the SMAHC bars

Bars/(Ni-Ti phase)	Theoretical Young's modulus	Experimental Young's modulus(1)	Percentage differences(2)
	E_{Theo} (GPa)	E_{Exp} (GPa)	(%)
1 (no wires)	11.380	10.317	+10.30
2 (SGA wires)	16.791	16.763	+ 0.17
3 (martensitic, 25 °C)	9.307	7.796	+19.38
4 (austenitic, 69 °C)	9.233	7.214	+27.99
5 (martensitic, 25 °C)	9.732	8.163	+19.22
6 (austenitic, 69 °C)	10.066	7.600	+24.45
7 (martensite, 25 °C)	10.577	10.510	+ 0.69
8 (austenitic, 69 °C)	12.823	12.810	+ 1.02
9 (austenitic, 69 °C)	13.045	7.280	+79.19

(1) measured at 25 ºC for bars 3, 5 ,7 and at 69 ºC for bars 4 , 6 , 8 and 9.
(2) the percentage values were calculated by the expression: $(E_{Theo} - E_{Exp} / E_{Exp}) \times 100$.

4. ANALYSES AND DISCUSSION OF RESULTS

4.1. General aspects of the fabrication of SMAHC beams and bars

The fabrication method incorporating a stretching device, developed in this study, worked satisfactorily at both cure temperatures, 25°C and 80°C, mainly with the Ni-Ti wires, relatively to the SGA wires, due to the fact that it was easier to keep the Ni-Ti wires stretched and well fixed at the extremities during the manufacturing process. Test specimens, including bars and beams, with volume fraction of E-glass fibers, V_f, in the range from 21% to 32,8% were obtained. Thus indicating that the operations of cutting as well as impregnation of the E-glass mat must be executed more carefully, in order to produce specimens with less variation in fiber content. Presently, instead of a vacuum bag, an external pressure of about 0.2 bar (0.02 MPa) is applied on the top surface of the male mould (which moves), by means of leaving heavy metal pieces on it during the consolidation of the composites. Additional specimens are being made, using vacuum bag during the cure of the epoxy matrix, but they were not tested yet. In the ´present process, part of the prepared resin (i.e. the excess) comes out from the mould and makes the extraction of the specimens rather difficult. So, attempts are being made to reduce the initial amount of resin, relatively to $\mathbf{m_f}$, from 1.5 to close to 1.

As far as the beams incorporating functional SMA wires are concerned, the manufacturing process produced specimens with very close values of thickness, mass as well as volume fractions of E-glass, wires and matrix (see beams 3 and 4 in Table 1), indicating that it produces SMAHC beams with repeatable characteristics. For the composite bars, the variations were higher. Finally, as shown in Fig. 9, the E-glass fibers do not touch the Ni-Ti wire, in bar 3 (see Table 2). The wire is surrounded by epoxy resin and voids were observed in the cross section of the bars and beams.

4,2. Elastic behavior of SMAHC beams in bending tests

As shown in Table 4, in general, the experimental values of the flexural modulus of the beams were always lower than the theoretical, by factors varying from about 55 % to 1.7 %. This suggests that the theoretical model, in which all interfaces are assumed to be perfect, overestimates the bending stiffness, of the specimens tested in this work. Considering the SMAHC beams (specimens 3 and 4), reinforced with Ni-Ti wires, it was noticed that for the tests at 69 ºC, both the theoretical as well as the experimental flexural modulus were higher than those of 25 ºC. This indicates, clearly, that the SMAHC with Ni-Ti wires in the austenitic phase are stiffer in bending. The increase in stiffness is moderate, but the volume fraction of wires in these specimens was in the range of only 1.7 to 1.8 %. The Ni-Ti wires are very expensive and difficult to incorporate in the composite beams. So, the strategy adopted in this investigation was to work only with up to 8 wires, in two layers of 4, but keeping such layers as far as possible from the middle surface of the SMAHC beams. The reason for this is the fact that, according to Eq. (1), in a laminated beam, the contribution of a generic ply (i) is proportional to $(z_i^3 - z_{i-1}^3)$, where z_i and z_{i-1} (see Fig. 7) are the distances from the middle plane, where a layer ends and begins, respectively (Gibson, 1994; Levy-Neto and Pardini, 2006). Thus, since z_i and z_{i-1} are in the third power, this non linear geometric effect amplifies the contribution of the plies which are located far from the middle plan and allows one to reduce costs and use, as effectively as possible, minimum amounts of Ni-Ti.

It was noticed that, theoretically, the beam without wires presented the maximum flexural modulus. The reason for this is the fact that in the layers with wires, 90% of the volume is epoxy resin and only the remaining 10% corresponds

to the wires. Thus, applying the rule of mixtures for this ply, both, for Ni-Ti wires at martensite and austenite phases, the longitudinal elasticity modulus is lower than that of the E-glass/epoxy ones.

4.3. Mechanical behavior of SMAHC bars in tension

For the SMAHC bars, the theoretical tensile elasticity moduli were also higher than the experimental values, as presented in Table 5, with differences varying from 0.69% to 28%. This indicates that the theoretical model overestimates the tensile stiffness of the bars tested in this work. And, although the bars incorporated up 6,04% in volume ($\mathbf{V_w}$) of Ni-Ti wires, the gains in stiffness were lower than those observed for the beams. For the bars, the number of wires varied from 2 to 8 and the gains in stiffness were expected to increase only linearly with increments of $\mathbf{V_w}$. In fact, since the E-glass/epoxy laminae and the Ni-Ti wires are all parallel to each other, the gain in tensile stiffness must follow, at least approximately, the rule of mixtures. The diagrams of Force versus displacement of an E-glass/epoxy (no wires) bar and a SMAHC bar with 8 wires are shown in Figs. 10.(a) and (b) , respectively. The diagrams are linear only in the beginning and, since the Ni-Ti wires present some ductility, the maximum elongation for the bar with 8 SMA wires was higher than the one for the E-glass/epoxy bar, by a factor larger than 2 times. For bars 3 and 4, with only 2 SMA wires (see Table 3), the elasticity modulus in tension (E) decreased when the temperature of the wires was increased from 25 ºC to 69 ºC. Only for the bars with 8 Ni-Ti wires there was a slight increase in E when the temperature increased from 25 ºC to 69 ºC. For the bars, in comparison with the beams, the variation in thickness was larger, maximum of 6.5%. So, improvements on the manufacturing of the bars are necessary.

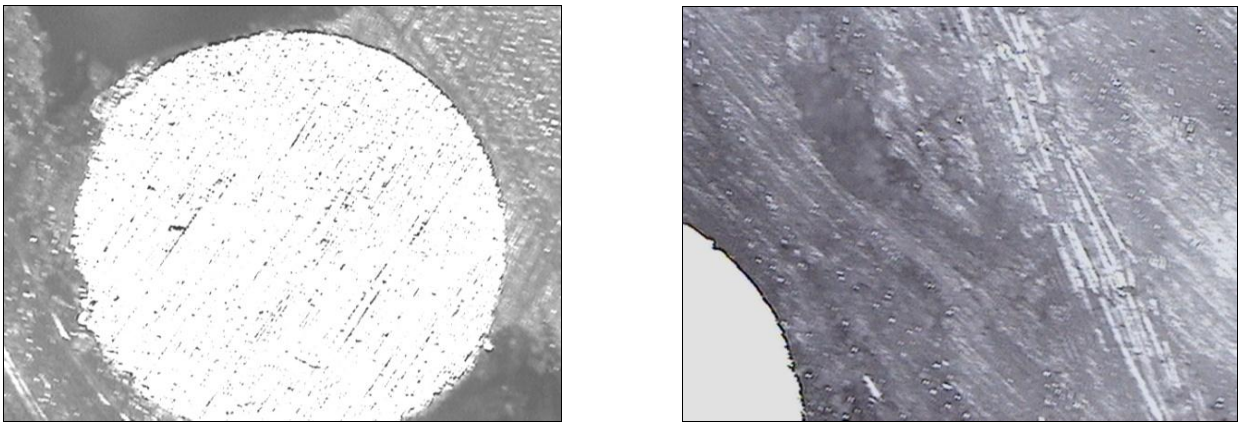

Figure 9. Micrograph of the cross section around a Ni-Ti wire (bar 3, 50 X).

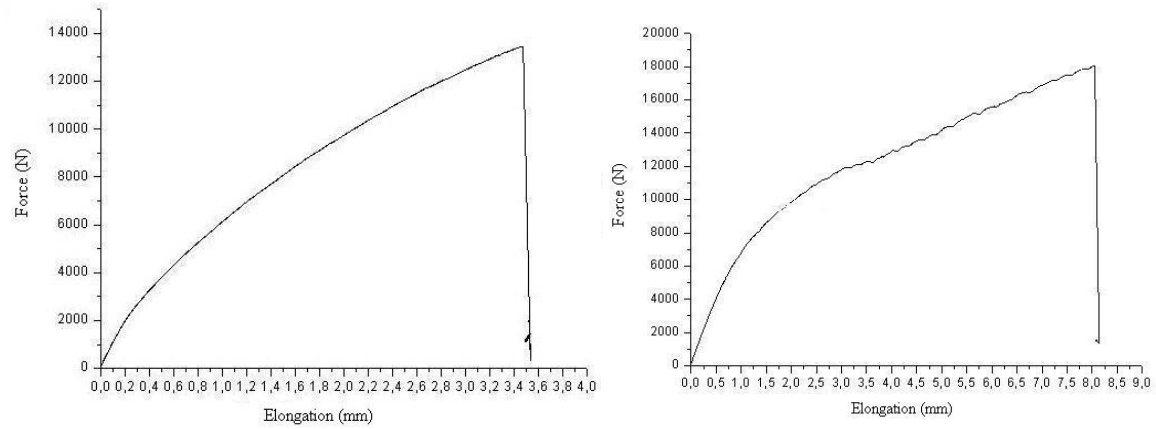

(a) Bar 2 without wires at 25 ºC (b) Bar 8 with 8 Ni-Ti wires at 69 ºC

Figure 10. Mechanical behavior of SMAHC bars: (a) without wires; and (b) with 8 Ni-Ti wires in tension.

5. MAIN CONCLUSIONS

An important conclusion regarding the SMAHC beams, as reported in Table 4, is the fact that the theoretical and experimental flexural modulus increased, from about 8.2% up to 11.5%, respectively, when the temperature of the wires increased from 25 ºC to 69 ºC. The maximum volume fraction of wires was 1.8% and an increment of 44 ºC increased the flexural modulus in at least 8.2%, indicating, clearly, that the bending stiffness can be controlled by means of the phase transformation of the Ni-Ti wires, from martensite to austenite, induced by the electric current.

For the SMAHC bars in tension, with volume fraction of Ni-Ti wires of 6.04%, the maximum increment in stiffness was 21.9%, when temperature is raised from 25 ºC to 69 ºC. Whereas for the SMAHC beams, with exactly the same variation in temperature, but with maximum volume fraction of Ni-Ti wires of only 1.8%, the increment obtained for the flexural modulus was 11.6%. In this regard, dividing the increments in stiffness by the respective volume fraction of Ni-Ti wires, these ratios are about **6.4** for the beams and **3.6** for the bars. This shows that both SMAHC components fabricated, modeled and tested in this work are promising to carry out vibration control in machines and structures by changing the stiffness with the phase transformation of the wires, but for the beams, the ratio of variation in stiffness over the amount of expensive SMA wires embedded is higher.

The fabrication process adopted, without vacuum bag, was satisfactory, mainly for the manufacturing of the SMAHC beams, which presented repeatable characteristics such as thickness, mass as well as volume fractions of matrix, E-glass and Ni-Ti wires.

6. ACKNOWLEDGEMENTS

The authors are grateful for the support they received from CNPq and Eletronorte.

7. REFERENCES

Castilho, W. S., 2008, “Thermomechanical characterization of Shape Memory Alloy Hybrid Composites”, Dissertação de Mestrado em Sistemas Mecatrônicos, Departamento de Engenharia Mecânica, Universidade de Brasília, Brasília, DF, 100p. (in Portuguese)

Cerón, D.M.S., 2010, “Development of a methodology for the fabrication of Shape Memory Alloy Hybrid Composites”, Dissertação de Mestrado em Ciências Mecânicas, Departamento de Engenharia Mecânica, Universidade de Brasília, Brasília, DF, 100p. (in Portuguese)

Daniel, I.M. and Ishai, O., 2006, "Engineering Mechanics of Composite Materials", Oxford University Press, Second Edition, Oxford, 411 p.

Faluhelyi, P., 2010, “Fabrication and Thermomechanical Behavior of Adaptative Structural Composite with Ni-Ti Filaments”, Doctorate Qualification, Department of Mechanical Engineering, University of Brasília, Brasília, DF. (in Portuguese)

Ghandi, M.V. and Thomson, B.S., 1992, “Smart Materials and Structures”, Chapman e Hall, London, 309 p.

Gibson, R.F., 1994, “Principles of Composite Material Mechanics”, McGraw-Hill Inc., New York. 425 p.

Janocha, H. (Editor), 1999, “Adaptronics and smart structures – Basics, materials, design and applications”. Springer – Verlag, Berlin Heidelberg, 438 p.

Levy, N. and Pardini, L.C., 2006, “Structural Composites, Science and Technology”, First Edition, Edgard Blücher, São Paulo, 313p. (in Portuguese)

Mendonça, P. T. R., 2005, “Composites Materials and Sandwich Structures”, Ed. Manole, 656p. (in Portuguese)

Otsuka K. and Wayman C. M., 1998, “Shape Memory Materials. Cambridge”. University Press.

Perkins, J., 1981, “Shape Memory Behavior and Thermoelastic Martensitic Transformations, Materials Science and Engineering, 51, p. 181-192.

Rogers, C.A. and Robertshaw, H.H., 1988, ”Shape Memory Reinforced Composites”, Engineering Science Preprints 23, ESP2588027, Society of Engineering Sciences.

Rogers, C. A., 1993, “Intelligent Material Systems–The Dawn of a New Materials Age”. Journal of Intelligent Materials System and Structures, Vol. 4, Technomic Publishing Company, Lancaster, U.S.A..

ScienceDirect. http://www.sciencedirect.com. Acessed in 20/04/2010.

Srinivasan, A.V. and McFarland, M. D. Smart Structures Analysis and Design, Cambridge University Press, 2001.

Turner, T.L., 2000, “Thermomechanical Response of Shape Memory Alloy Hybrid Composites”. NASA/TM-2001-210656, Langley Research Center, Hampton, Virginia, 2000.

Wayman, C. M., Duerig, T. W. Engineering Aspects of Shape Memory Alloys. Eds.: Duerig, T.W., Melton, K. N.,Stockel, D., Wayman, C. M. Butterworth-Heinemann. p. 3-20. 1990.

Zak, A.J.; Cartmell, M.P.; Ostachowicz, W. M. Dynamics and control of a rotor using an integrated SMA/composite active bearing actuator. Key Engineering Materials, Switzerland, v. 245-246, p. 233-240, 2003.

Zheng, Y., Cui, L.; Schrooten, J.. Thermal cycling behaviors of a NiTiCu wire reinforced Kevlar/epoxy composite. Materials letters, v. 59, p. 3287- 3290, 2005.

8. RESPONSIBILITY NOTICE

The authors are the only responsible for the printed material included in this paper.